COBEM 2023 27TH INTERNATIONAL CONGRESS OF MECHANICAL ENGENEERING

ABCM Brazilian Society of Mechanical Sciences and Engineering
27th ABCM International Congress of Mechanical Engineering
December 04-08, 2023, Florianópolis-SC, Brazil

COB-2023-1373
2-DOF DISCRETE MODEL FOR NON-LINEAR VIBRATIONS ANALYSIS OF GUYED TOWERS CONSIDERING UNILATERAL CONTACT CABLES

Fernanda Neves da Silva
Frederico Martins Alves da Silva
School of Civil Engineering, Federal University of Goiás, UFG
Av. Universitária, n.º 1488 - quadra 86 - Setor Leste Universitário, 74605-010, Goiânia, Goiás, Brasil
fernanda_neves@discente.ufg.br, silvafma@ufg.br

Abstract. *Guyed structural systems are commonly used in different engineering areas, but their designs are heavily dependent on stability criteria due to their high slenderness ratio. The cables used in these structures are highly efficient when tensioned, which allows them to absorb a significant portion of the loads acting on the structures. However, accidents involving cable-stayed towers are not uncommon, with cable rupture being a frequent cause of structural failure. In this study, we aim to analyze the statical and dynamical nonlinear behavior of a discrete plane guyed tower model by a two degrees of freedom model. We also pay special attention to the effect of unilateral constraints on the nonlinear displacements of the guyed tower. Unilateral constraints are critical in this type of application as they affect the capacity of the stays to resist only the tensile efforts, which modifies the statical and dynamical analysis of the proposed structural system. To account for geometric nonlinearity, we define the equilibrium equations by observing the deformed configuration equilibrium under the action of external loads and prestressing in the cables. We carry out a parametric analysis of the influence of the unilateral contact of the stays on the critical load, the post-critical behavior, and in the nonlinear vibrations. Our findings reveal a significant influence of the consideration of unilateral constraints on the statical and dynamical stability of the model, leading to a marked decrease in the critical load of the structure and changing the dynamical bifurcation diagrams, suggesting that geometric nonlinearities and the restriction of the contact of stays significantly affect the nonlinear behavior of this type of structure, and these effects must be taken into account in the design step.*

Keywords: *Nonlinear dynamics, Guyed towers, Unilateral constraints.*

1. INTRODUCTION

The improvement of construction techniques, associated with the use of new materials and the development of new technologies, has resulted in projects of increasingly slenderness and flexible structures. Guyed structural systems contain these aspects and are widely used in many engineering applications. As the structural elements are designed with greater slenderness, the structure becomes more susceptible to lateral vibrations. Thus, as evidenced by Del Prado et al. (2010), geometric nonlinearities are associated with their static and dynamic behavior. Carvalho (2008) reports that the efficiency of cable-stayed structures to support axial loads is due to the presence of cable elements, which present high efficiency when subjected to traction, fully meeting the required architectural and structural concepts.

Del Prado et al. (2010) and Ballaben et al. (2017) investigate a guyed tower structure model under wind loading. The authors found that the pre-tension of the cables is the most important parameter in the analysis of the dynamic transverse displacements of the structure. Marques et al. (2021) and Cucuzza et al. (2022) analyze the effects of geometric nonlinearities and the influence of cable on the response of the static and dynamic structure of a continuous structural model of a guyed tower. The results indicate that the studied model presents a highly non-linear response, even under low load levels, therefore, this must be considered carefully in the design. The uniform distribution of cables can give rise to coincident buckling loads and vibration frequencies (Marques at al., 2021). Giving the importance of cable analysis, Sequeira et. al (2022) report that many accidents occur in guyed towers due to cable rupture. Thus, the authors investigate the sudden rupture of one or two cables, arbitrarily selected, in the linear and non-linear response of the guyed tower under static and dynamic loads of a tower model studied via finite elements. The results show that this type of structure is sensitive to physical and geometric nonlinearities and to rupture, indicating that this cable rupture should be considered in the design of the tower structure because the cable failure produces a reduction in buckling load and vibration.

According to Barbosa (1986), some structures may be in unilateral contact, which are boundary conditions that resist the displacements of bodies only in certain directions or prevent such displacements. In this context, it is noteworthy that guyed towers are a class of structures in which the consideration of the hypothesis of unilateral contact of the cables - which resist the displacements of the tower if tensioned - must be considered to obtain a more accurate mathematical model. In this sense, this work intends to investigate the unilateral contact (boundary condition) in the non-linear oscillations of guyed towers. The unilateral contact is manifested in this type of application from the consideration of the

capacity of the cables resist only the tensile forces, which strongly modifies the static and dynamic analysis of the proposed structural system. From this contextualization, the analysis of stability and non-linear vibrations of guyed towers is carried out, considering the unilateral contact of cables in the equivalent mathematical model.

2. MATHEMATICAL FORMULATION

Consider a discrete plan tower model with a central mast comprising two pinned rigid bars. The lower bar of length h_1 has a rotational spring at its lower end, and a spring at the upper end that connects it to a consecutive rigid bar of length h_2. The lateral displacements are restricted by translational linear springs, representing the cables and responsible for ensuring the stability of the structure. These springs with stiffness coefficients k_1, k_2, k_3 and k_4 are fixed at anchor points arranged at a distance L from the tower. The tower is subjected to four loads, being an axial load P and a concentrated mass m applied at the end of the tower, and axial loads p_1 and p_2, corresponding to the self-weight of the bars of length h_1 and h_2, respectively. The system has two rotational degrees of freedom denoted by θ_1 and θ_2, that represent the rotations associated with rotational springs with stiffness coefficients $k_{\theta 1}$ and $k_{\theta 2}$, respectively. Therefore, each bar has a unique degree of freedom, and the structure is characterized by the series of these two variables that uniquely determine its position in the deformed configuration. In Figure 1(a), the tower is shown in the fundamental equilibrium configuration while Figure 1(b) presents the deformed configuration of the structure.

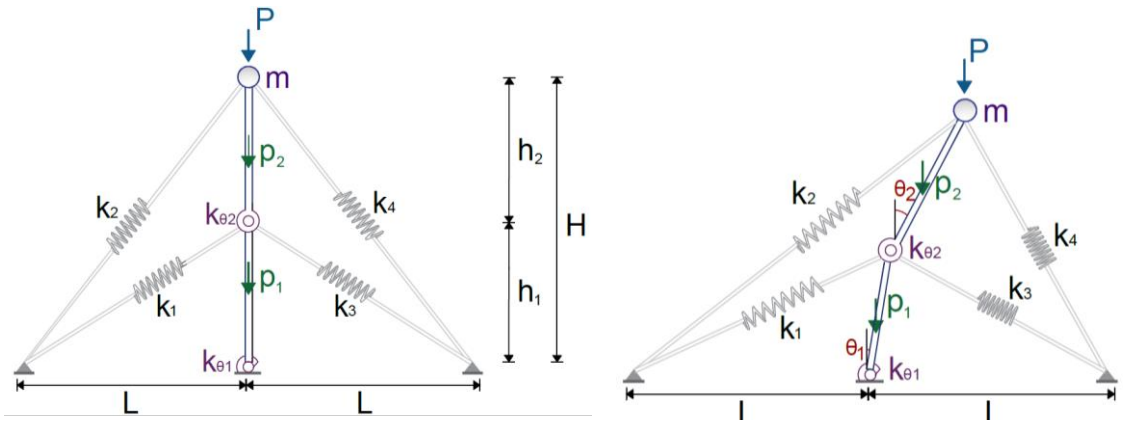

(a) initial configuration (b) deformed configuration

Figure 1. Geometric model in (a) initial and (b) deformed configuration.

The structural stability is based on the energy criterion that relates the internal energy of deformation and the work done by the external forces of the structure. The variation of the spring length, Δl_{i}, is expressed by the sum of an initial cable elongation Δl_0, caused by the prestressing force acting on the springs, and a cable elongation, Δl_P, that it is a function of the rotations of the bars when they undergo the action of external load. Then Δl_{i} is written in the form:

$$\Delta l_i = (\Delta l_0)_i + (\Delta l_P)_i, \tag{1}$$

where the elongation due to the prestressing of the stays is given by:

$$(\Delta l_0)_i = -(F_0)_i \,/\, k_i. \tag{1}$$

It is noteworthy that the angles θ_1 and θ_2 are considered positive in the direction of rotation indicated by Figure 1b. The expressions of Δl_P, when calculating the variation between the final and initial lengths of the four analyzed springs and considering the proposed rotation, are given by:

$$\Delta l_{p_1} = \sqrt{h_1^2 + 2\,L\,h_1\,sin\,\theta_1 + L^2} - \sqrt{h_1^2 + L^2}\,, \qquad \Delta l_{p_3} = \sqrt{h_1^2 - 2\,L\,h_1\,sin\,\theta_1 + L^2} - \sqrt{h_1^2 + L^2},$$

$$\Delta l_{p_2} = \sqrt{h_1^2 + h_2^2 + 2\,h_1\,h_2\,cos(\,\theta_2 - \theta_1) + 2\,L\,(h_2\,sin\,\theta_2 + h_1\,sin\,\theta_1) + L^2} - \sqrt{H^2 + L^2}, \tag{3}$$

$$\Delta l_{p_4} = \sqrt{h_1^2 + h_2^2 + 2\,h_1\,h_2\,cos(\,\theta_2 - \theta_1) - 2\,L\,(h_2\,sin\,\theta_2 + h_1\,sin\,\theta_1) + L^2} - \sqrt{H^2 + L^2}.$$

The internal deformation energy of the system considers the contributions of the energy referring to each translational spring, and the related rotational springs. The work of external loads considers the effects of loads P, p_1, p_2 and the concentrated mass m applied to the structure. So, the sum of these energies results in the variation of the total potential energy:

$$\Delta\pi = \frac{1}{2}\sum_{i=1}^{4} FS_i\, k_i\, (\Delta l_{0i} + \Delta l_{pi})^2 + \frac{1}{2}\, k_{\theta 1}\, \theta_1^2 + \frac{1}{2}\, k_{\theta 2}\, (\theta_2 - \theta_1)^2 - p_1\left(\frac{h_1}{2} - \frac{h_1\, cos\,\theta_1}{2}\right) - p_2\left(H - \frac{h_2}{2} - h_1\, cos\,\theta_1 - \frac{h_2\, cos\,\theta_2}{2}\right) - (P + m\, g)\,(H - h_1\, cos\,\theta_1 - h_2\, cos\,\theta_2), \tag{4}$$

where the parameter FS_i represents the *Signum* function, introducing in this formulation the consideration of unilateral contact. This function is a mathematical consideration that extracts the sign of a real or complex number and, when applied to the terms of the internal deformation energy referring to the springs, fulfills the objective of disregarding such elements subjected to compression. In this context, to perform an analysis that considers the unilateral contact, FS_i must assume the following expressions:

$$FS_{\mathrm{i}} = \left(\frac{signum\,(\Delta l_{0i} + \Delta l_{pi})}{2} + \frac{1}{2}\right), i = 1, 2, 3, 4. \tag{5}$$

However, for an analysis that does not consider this restriction of unilateral contact, that is, the effects of all springs will be accounted in the study of the behavior of the structural system (bilateral contact), FS_i must assume a unit value.

The system of nonlinear statical equilibrium equations is obtained by deriving the expression of the total potential energy, indicated by Eq. (4), as a function of the generalized coordinates, θ_1 and θ_2:

$$\frac{1}{2}\sum_{i=1}^{4}\left[FS_i \frac{\partial}{\partial\theta_1}\left(k_i\,(\Delta l_{0i} + \Delta l_{pi})^2\right)\right] - \frac{p_1\, h_1\, sin\,\theta_1}{2} - p_2\, h_1\, sin\,\theta_1 + k_{\theta 1}\,\theta_1 - k_{\theta 2}\,(\theta_2 - \theta_1) - (P + \alpha\, m\, g)\, h_1\, sin\,\theta_1 = 0, \tag{6}$$

$$\frac{1}{2}\sum_{i=1}^{4}\left[FS_i \frac{\partial}{\partial\theta_2}\left(k_i\,(\Delta l_{0i} + \Delta l_{pi})^2\right)\right] - \frac{p_2 h_2\, sin\,\theta_2}{2} + k_{\theta 2}\,(\theta_2 - \theta_1) - (P + \alpha\, m\, g)\, h_2\, sin\,\theta_2 = 0. \tag{7}$$

The statical equilibrium path of the system is determined using the standard Newton-Raphson method to solve the equations (6) and (7), obtaining a series of values for P, θ_1 and θ_2 that represent the non-linear equilibrium trajectory.

To obtain the nonlinear dynamical equation, the Lagrangian approach is used, involving the kinetic energy and the total potential energy. Obtaining the kinetic energy - that comprises two rigid bars with the density of the material, ρ, and that the cross-sectional area, A - the nonlinear damped equilibrium equations assume the form indicated by Eqs. (8) and (9).

$$\left(\frac{\rho\, A\, h_1^3}{3} + m\, h_1^2\right)\ddot{\theta}_1 + (m\, h_1\, h_2\, cos(\theta_1 - \theta_2))\,\ddot{\theta}_2 + 2\left(\frac{\rho\, A\, h_1^3}{3} + \frac{\rho\, A\, h_2^3}{3}\right)\omega\,\xi\,\dot{\theta}_1 + \frac{d\Delta\Pi}{d\theta_1} = 0, \tag{8}$$

$$(m\, h_1\, h_2\, cos(\theta_1 - \theta_2))\,\ddot{\theta}_1 + \left(\frac{\rho\, A\, h_2^3}{3} + m\, h_2^2\right)\ddot{\theta}_2 + 2\left(\frac{\rho\, A\, h_1^3}{3} + \frac{\rho\, A\, h_2^3}{3}\right)\omega\,\xi\,\dot{\theta}_2 + \frac{d\Delta\Pi}{d\theta_2} = 0. \tag{9}$$

The second order differential equations set, Eqs. (8) and (9), are transformed into a system of first order differential equations of motion. Then these systems are integrated in time using the 4th order Runge-Kutta method. It is important to notice that from the set of first order differential equations of motion, a Jacobian matrix can be obtained. The classification of equilibrium points is determined by the eigenvalues λ_1, λ_2, λ_3 and λ_4 of the Jacobian matrix. Ricardo (2009) approaches the classification of the stability of fixed points from the numerical characteristic of λ_i. According to the author, if all the eigenvalues have the real parts equal to zero, and the imaginary parts are not zero, there is a stable center. If all the eigenvalue real parts are negative, the point is stable, and if at least one eigenvalue has a positive real part, it is classified as unstable. A node and a focus are different equilibrium points where the first one all imaginaries parts of eigenvalues must be null while the focus has its imaginary part of eigenvalues not null. The saddle is characterized by having real eigenvalues with opposite signs.

In this work, the nonlinear dynamic analysis of forced vibration is performed by assuming that the load P is a time-dependent function, that is, it is considered that the tower is excited by a harmonic axial load in the form:

$$P = \mathrm{F}_1 + \mathrm{F}_2 \cos(\Omega\, t), \tag{10}$$

where F_1 and F_2 are threshold load ratios, and Ω is the harmonic loading excitation frequency.

The brute-force numerical method was used to obtain the bifurcation diagrams due to its programming simplicity and its scope to find several types of solutions, such as fixed points, periodic solutions, quasi-periodic solutions and chaotic motions. Basically, in the brute force method, to identify the attractor associated with a given control parameter, a set of initial conditions is chosen and the system is integrated for a sufficiently long time to arrive at the Poincaré mapping of the permanent response (Del Prado, 2001).

3. NUMERICAL RESULTS

To obtain the numerical results, the following values corresponding to the parameters involving the model were considered: $h_1 = h_2 = 5\ m, H = 30\ m, L = 15\ m, p_1 = p_2 = 4.9$ kN, $k = 50\ kN/m$, $F_0 = 5$ kN, m = 1000 kg, g = 9.81 m/s^2, $k_{\theta 1} = 10\ kN/rad$ and $k_{\theta 2} = 10\ kN/rad$.

3.1 Nonlinear Static Analysis

Figure 2 shows the nonlinear equilibrium path of the structural system under bilateral contact, projected in the two orthogonal planes, $P \times \theta_1$ and $P \times \theta_2$. The continuous lines correspond to the stable equilibrium configurations and the dashed lines to the unstable configuration.

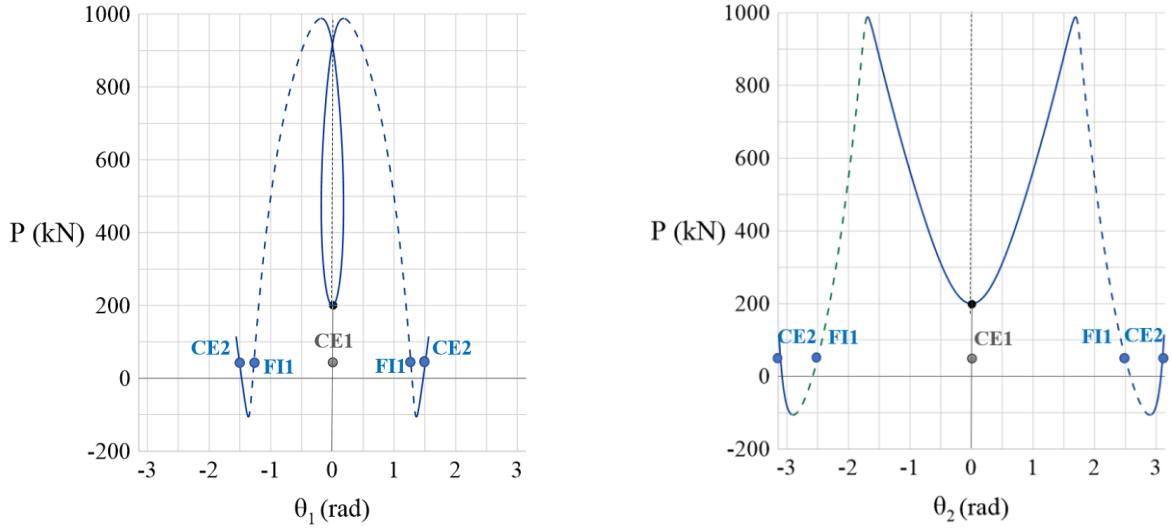

(a) $\lambda \times \theta_1$ plane (b) $\lambda \times \theta_2$ plane

Figure 2. Post critical path (bilateral contact): (a) in the $\lambda \times \theta_1$ plane (b) in the $\lambda \times \theta_2$ plane.

As expected, due to the symmetry of the system, the right and left branches of the nonlinear statical equilibrium path are equal and there is the presence of a critical load (bifurcation point) in the fundamental equilibrium path ($\theta_1 = \theta_2 = 0$). As the compressive load increases, a non-linear stable path is observed with increasing effective stiffness up to the first maximum limit point. The limit point is followed by an expressive decreasing in stiffness until a minimum point, and from this, the stiffness increases again. In this work, the load parameter $P = 40$ kN was adopted, in order to classify all points along the non-linear trajectory of equilibrium submitted to this load. Note that there are five static equilibrium configurations corresponding to this load: a center corresponding to the stable equilibrium position along the fundamental path (CE1 – Stable Center 1), two unstable focus equilibrium along the path (FI1 – Unstable Centers 1), and two centers related to stable equilibrium positions (CE2 – Stable Centers 2).

Considering the unilateral contact of the stays, the non-linear equilibrium paths are shown in Figure 3. Analogously, to the post-critical path obtained for the bilateral contact, it is noted that the non-linear equilibrium trajectories along the displacements are symmetrical. However, in this case there is no presence of critical loads, therefore, the non-linear equilibrium path has a limit point associated with the rotations θ_1 e θ_2 ($P_{lim} = 52\ kN$). It is noteworthy that P_{lim} is lower than the critical load obtained in the analysis of the system with bilateral contact, given by $P_{cr} = 200$ kN. Therefore,

when considering the unilateral contact, it is found that there is a considerable decrease in the load that causes the process of loss of stability due to the loss of stiffness of the structural system.

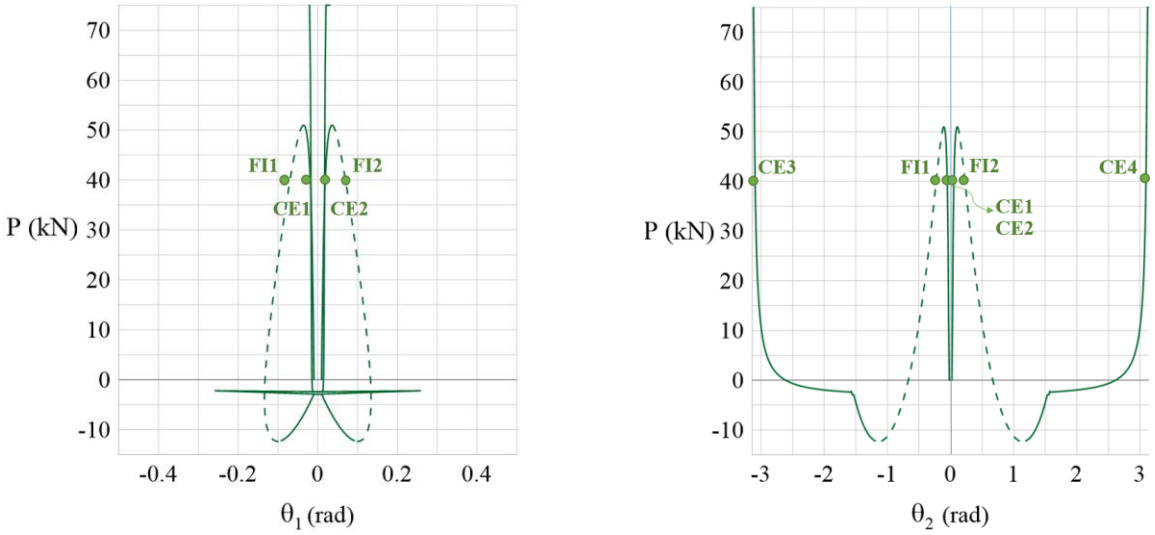

(a) $\lambda \times \theta_1$ plane (b) $\lambda \times \theta_2$ plane

Figure 3. Post critical path (unilateral contact): (a) in the $\lambda \times \theta_1$ plane (b) in the $\lambda \times \theta_2$ plane.

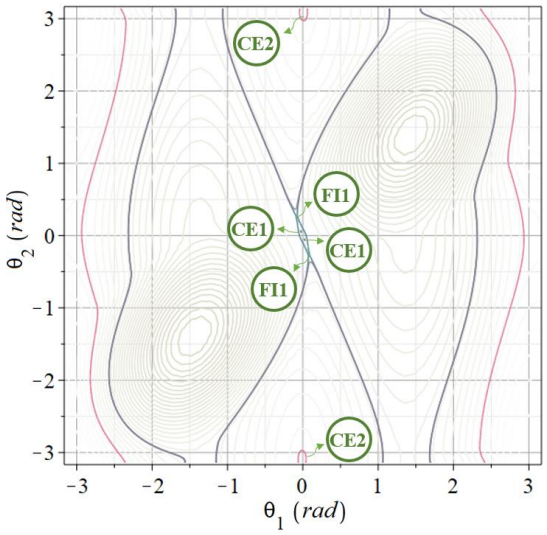

Figure 4. Potential energy surface curves (unilateral contact).

When comparing the trajectories presented for the two forms of contact of stays, as shown in Figure 2 (bilateral) and in Figure 3 (unilateral), it is notable that the stable path do not precisely comprise the same interval in both cases, since few stable intervals are correspondents. For unilateral contact, there is a greater restriction for displacements related to θ_2 compared to bilateral contact. On the other hand, there are larger intervals of stable θ_1 in the case where unilateral contact is considered. The destaked points for the load parameter $P = 40\ kN$, indicated in Figure 3, as well as in the potential energy surface curves for the same case are shown in Figure 4. Note the existence of six static equilibrium configurations for the analyzed load: two centers corresponding to stable equilibrium positions under small displacements (CE1), two focus related to unstable equilibrium positions along the trajectory (FI1) and two related centers to stable equilibrium positions with large displacements of θ_2 (CE2). The classification of these points is carried out based on the analysis of the study of stability according to Lyapunov.

3.2 Nonlinear Dynamic Analysis

In order to carry out the investigation of nonlinear oscillations and dynamic instability of a discrete guyed tower system that considers unilateral contact, some nonlinear dynamics tools are used, such as phase portraits and bifurcation diagrams. From the analysis of Figure 3, the unilateral contact modifies the statical nonlinear behavior of the guyed tower, and it is expected important changes in the dynamic nonlinear behavior of this same tower.

For structures under dynamical loads, it is important to carry out a detailed study of the system response in the space of the control parameters to detect the unstable regions. The following parameters are adopted: $\xi = 0.01, A = 0.1\ m^2$ e $\rho = 0.01\ kg/m^3$. Initially, the natural frequencies of the discrete guyed tower model are evaluated. For this, the dynamical equilibrium equations, Eqs. (8) and (9), are linearized around the vertical position of the tower ($\theta_1 = \theta_2 = 0$), and then the degrees of freedom are discretized in time as $\theta_1 = \overline{\theta_1}\cos(\omega t)$ and $\theta_2 = \overline{\theta_2}\cos(\omega t)$, leading to an eigenvalue problem where ω is the natural frequency of the discrete model. In this way, the natural frequencies $\omega_b = 7{,}07\ rad/s$ e $\omega_u = 4{,}62\ rad/s$ are obtained for the bilateral and unilateral contact, respectively. When comparing the natural frequency values for these two cases of contact, it is observed that the tower model subjected to bilateral contact has a higher natural frequency compared to the model that considers unilateral contact. As some cables can be disregarded during free vibration due to the unilateral contact of the stays, there is a decrease in the global stiffness of the structure and, for this reason, the natural frequency is also reduced.

It is considered that the guyed tower is subjected to a harmonic axial load, as presented by Eq. (10). The term referring to the static force of this load is considered $F_1 = 0{,}4\ P_{cr}$, for the case in which bilateral contact, or $F_1 = 0{,}4\ P_{lim}$ for the analysis of unilateral contact. An analysis of the bifurcation diagrams corresponding to the excitation frequency $\Omega = 1\omega_b$, or $(1\omega_u)$, for the bilateral and unilateral contact, respectively, are presented by Figures 5a and 5b. The bifurcation diagrams, with emphasis on the solutions of θ_1, around the vertical position of the tower mast, are obtained through the brute force algorithm, and have as control parameter the amplitude of the dynamic force, F_2. Figure 5a indicates that by increasing the amplitude of the dynamic force, the permanent response tending to the trivial solution (rotations equal to zero) starts to present multiple periods as well as it loses stability and jumps to a non-trivial stable solution with a greater amplitude of vibration. The equilibrium path in blue is symmetrical to the equilibrium path in red. It is noteworthy that Figure 5 displays only the bifurcation diagram of θ_1 because the sequence of bifurcation for θ_2 is the same. So, for simplicity and brevity to show the numerical results, we decided to present only the first bifurcation diagrams.

Regarding the analysis of unilateral contact, it is observed that there are no trivial solutions, since the system is characterized by absence of fundamental path in these cases. Note that, when varying the values of F_2, the bifurcation diagram, shown in Figure 5b, presents several bifurcation points with sequences of branches with periodic, quasi-periodic and chaotic vibrations. In terms of complexity and variety of dynamical solutions presented in the bifurcation diagram, the unilateral contact of the stays causes a behavior similar to the case of the bilateral contact of the stays. However, for small values of F2, the absence of trivial solution is the main change provoked by the unilateral contact.

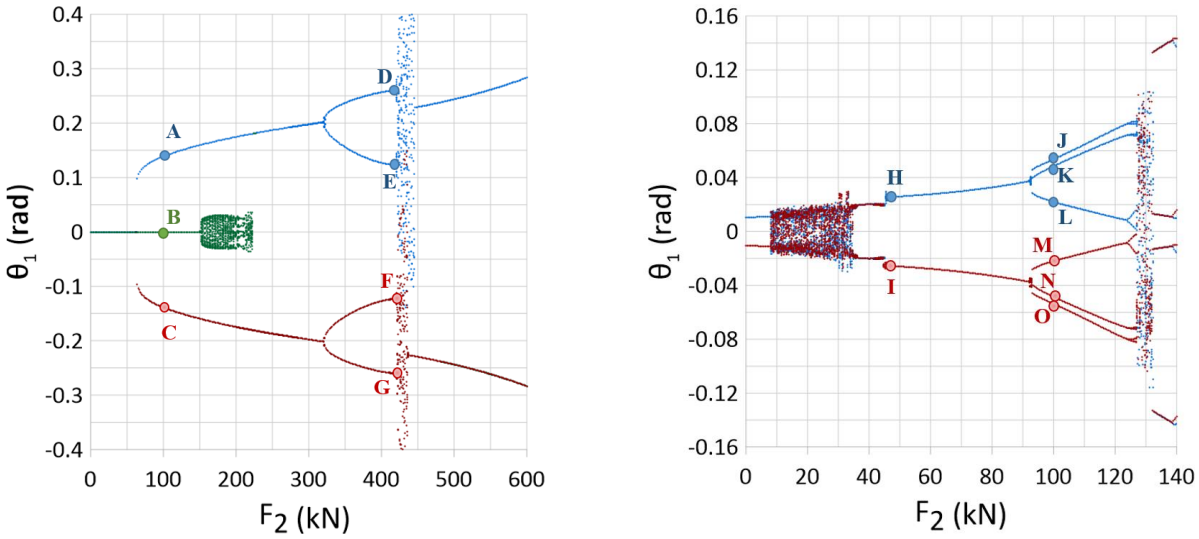

(a) bilateral contact (b) unilateral contact

Figure 5. Bifurcation diagrams for (a) bilateral contact (b) unilateral contact

In Figures 6a and 6b, the phase portraits and the Poincaré sections of the points present in the bifurcation diagrams of Figure 5 are illustrated. The same value of F_2 is considered in order to compare the phase portraits of the two hypotheses of stays contact. The chosen value is $F_2 = 100\ kN$. Figure 6a shows that the tower with bilateral contact assumes two

non-trivial stable solutions of period 1T, indicated by the Poincaré sections A and C, and one trivial solution B. However, the phase portrait of tower with unilateral contact, Figure 6b, indicates the presence of two stable responses of period 3T for the permanent dynamical response. In other words, the dynamical behavior is strongly affected by the unilateral contact hypothesis. The same behavior were observed in the plane $\theta_2 x d\theta_2/dt$ and it can be omitted without losing relevant information about dynamic behavior.

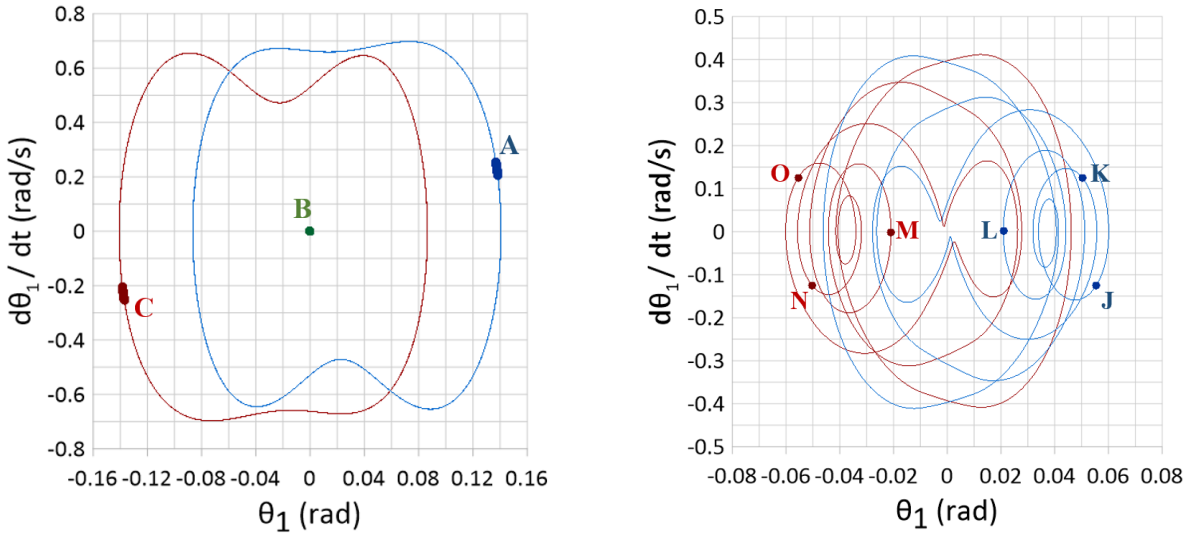

(a) bilateral contact (b) unilateral contact

Figure 6. Phase plan and Poincaré Map for $F_2 = 100\ kN$ considering (a) bilateral contact (b) unilateral contact

Figure 7a shows that multi-period responses, represented by the Poincaré sections D, E, F and G, Figure 5a, are obtained in the region around $F_2 = 420\ kN$. These answers obtained through the consideration of bilateral contact show the presence of quasi-periodic solutions. The quasi-periodic responses also are found for the bifurcation diagram related to unilateral contact, as shown in Figure 7b, referring to the phase portrait of sections H and I, as illustrated in Figure 7b.

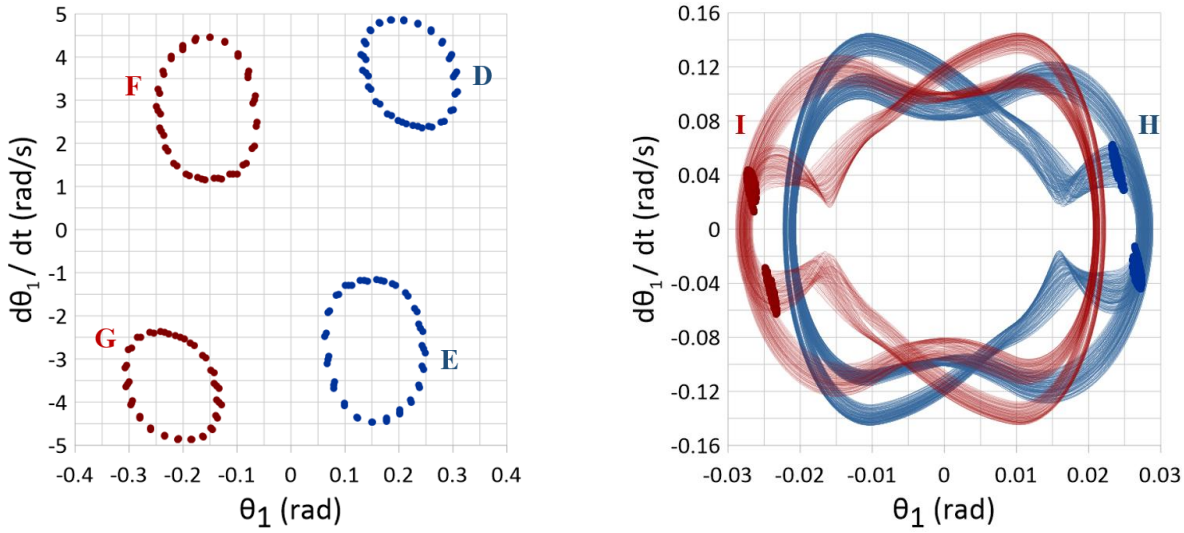

(a) $F_2 = 420\ kN$ (bilateral contact) (b) $F_2 = 46\ kN$ (unilateral contact)

Figure 7. Poincaré Map for (a) $F_2 = 420\ kN$ (bilateral contact) (b) $F_2 = 46\ kN$ (unilateral contact)

4. CONCLUSIONS

A mathematical discrete model capable of considering only the cables that are effectively tensioned was developed for a discrete plan guyed tower system. The presence of static loads and, mainly, dynamic loads in nonlinear structural systems, such as the investigated tower model, are factors that make a meticulous analysis of the behavior of these

structures necessary. As evidenced in the static and dynamic results, the consideration of unilateral contact in the analysis of the stability of the structural system is responsible for strongly changes in the nonlinear equilibrium responses, since there is a considerable loss of stiffness of the structural system.

5. ACKNOWLEDGEMENTS

This work was made possible by the support of the Brazilian research agency CNPq, CAPES and FAPEG (Fundação de Apoio e Amparo à Pesquisa do Estado de Goiás).

6. REFERENCES

Ballaben, J. S.; Guzmán, A. M.; and Rosales, M. B, 2017. *Nonlinear dynamics of guyed masts under wind load: Sensitivity to structural parameters and load models*. Journal of Wind Engineering and Industrial Aerodynamics, v. 169, p. 128-138.

Barbosa, H. J. C, 1986. *Numerical algorithms for contact problems in elasticity (in Portuguese).* Ph.D. thesis, COPPE-UFRJ, Rio de Janeiro, Brazil.

Carvalho, E. C, 2008. *Dynamic Instability Analysis of Guyed Structures (in Portuguese)*. Master's thesis. Universidade Federal de Goiás.

Cucuzza, R.; Rosso, M. M.; Aloisio, A.; Melchiorre, J.; Giudice, M. L.; and Marano, G. C, 2022. *Size and Shape Optimization of a Guyed Mast Structure under Wind, Ice and Seismic Loading.* Applied Sciences, 12(10), 4875.

Del Prado, Z. J. G. N, 2001. *Modal coupling and interaction in the dynamic instability of cylindrical shells*. D. Sc. Thesis, Civil Engineering Department, Catholic University, PUC-Rio. Rio de Janeiro, RJ, Brazil.

Del Prado, Z. J. G. N; Carvalho, E. C.; and Gonçalves, P. B, 2010. *Dynamic stability of imperfect cable stayed masts*. Mecánica computacional, v. 29, n. 7, p. 647-658.

Marques, Í. R.; Gonçalves, P. B.; and Roehl D. M, 2021. Effect of the cable system on the static and dynamic stability of Guyed Towers. *III Pan-American Congress on Computational Mechanics*.

Ricardo, H. J, 2020. *A modern introduction to differential equations*. Academic Press.

Sequeira, L. E. F.; Gonçalves, P. B.; and Roehl, D, 2022. *Assessment of the Elastoplastic Nonlinear Static and Dynamic Behavior of Guyed Antenna Towers Subjected to Cable Rupture*. ce/papers, v. 5, n. 4, p. 755-763.

7. RESPONSIBILITY NOTICE

The author(s) is (are) the only responsible for the printed material included in this paper.